Nanophase-Separated Blends of Acceptor and Donor Conjugated Polymers. Efficient Electroluminescence from Binary Polyquinoline/Poly(2-methoxy-5-(2′-ethylhexyloxy)-1,4-phenylenevinylene) and Polyquinoline/Poly(3-octylthiophene) Blends

Maksudul M. Alam, Christopher J. Tonzola, and Samson A. Jenekhe*

Department of Chemical Engineering and Department of Chemistry, University of Washington, Seattle, Washington 98195-1750

Received May 14, 2003; Revised Manuscript Received June 15, 2003

ABSTRACT: Binary blends of the acceptor conjugated polymer poly(2,2′-(3,3′-dioctyl-2,2′-bithienylene)-6,6′-bis(4-phenylenequinoline)) (POBTPQ) with donor conjugated polymer poly(2-methoxy-5-(2′-ethylhexyloxy)-1,4-phenylenevinylene) (MEH−PPV) or poly(3-octylthiophene) (POT) were nanophase-separated and observed to exhibit efficient electroluminescence in light-emitting-diodes. The 90−120 nm phase-separated morphology of MEH−PPV-containing blends was characteristic of dimixing by spinodal decomposition whereas that of POT-containing blends consisted of nucleation and growth type spherical domains (50−400 nm) dispersed in a matrix. Efficient Förster energy transfer was observed in both blend systems. Voltage-tunable orange-red ↔ yellow ↔ green electroluminescence was observed in the POBTPQ:MEH−PPV blend diodes at a composition of 10−80 wt % MEH−PPV. Only red emission characteristic of POT was observed from POBTPQ:POT blend devices due to efficient energy transfer from POBTPQ. Large enhancements in performance of the bipolar blend light-emitting diodes were observed compared to that of the homopolymer diodes. The compositional dependence of luminance and external quantum efficiency of the blend devices was very different for the MEH−PPV and POT blends, reflecting the difference in morphology. Electric-field-induced photoluminescence quenching confirmed the bipolar charge transport in the blends and associated improved electron−hole recombination and device efficiencies. These results demonstrate that efficient electroluminescence can be achieved in bipolar blends of conjugated polymers and that nanophase-separated morphology is essential to voltage-tunable multicolor light emission in blend devices.

Introduction

Conjugated polymer semiconductors have useful electronic, optoelectronic, and photonic properties which are currently being exploited in various device applications,[1−9] including light-emitting diodes,[1−3] photovoltaic cells,[4,5] thin film transistors,[6,7] and electrochromic cells.[8] Because novel phenomena and *supramolecular properties* not found in the constituent homopolymers can emerge in blends of conjugated polymers due to intermolecular interactions, self-organization, and confinement effects, they are of fundamental and technological interests.[9] Supramolecular properties that have previously been reported in blends of conjugated polymers include ground-state charge transfer,[10] photoinduced charge transfer,[4,11] exciplex formation,[12] energy transfer,[13] enhanced charge transport,[7b,c] and exciton confinement.[9,14] The extent to which any of these supramolecular properties occurs in a given blend system depends on the electronic structures (HOMO/LUMO levels) of the conjugated polymer components, the dominant intermolecular interactions, and the self-organization and hence the morphology. Systematic studies of these rich features of blends of conjugated polymers will allow their development into useful technological materials for electronics and photonics.

Electroluminescence from blends of emissive conjugated polymers has been reported.[9,13] However, all of the prior blends of electroluminescent polymers have been *unipolar* in the sense that the components were of the same type: either *all-p-type* blends[13a−c] exemplified by poly(3-hexylthiophene)/poly(2-methoxy-5-(2′-ethyl-hexyloxy)-1,4-phenylenevinylene) (MEH−PPV) system[13b] or *all-n-type* blends such as binary blends of two different polyquinolines.[9] Few studies of blends of acceptor (n-type) and donor (p-type) conjugated polymers have been reported.[4,10] Prior reports of such blends of donor and acceptor conjugated polymers showed that they generally undergo photoinduced charge transfer and separation, leading to quenching of electroluminescence and enhancement of photovoltaic properties.[4] Photovoltaic cells have thus been fabricated from blends of p-type (hole accepting) poly(2-methoxy-5-(2′-ethylhexyloxy)-1,4-phenylenevinylene) (MEH−PPV) with n-type (electron accepting) cyano-substituted poly(phenylenevinylene) (CN−PPV)[4a] and from blends of p-type poly(9,9′-dioctylfluorene-*co*-bis-*N*,*N*′-(4-butylphenyl)-bis-*N*,*N*′-phenyl-1,4-phenylenediamine) (PFB) with n-type poly(9,9′-dioctylfluorene-*co*-benzothiadiazole) (F8BT).[4c] Bipolar conductivity was observed from a binary blend of p-type polypyrrole with n-type ladder poly(benzimidazole−benzophenanthroline) (BBL).[10] To our knowledge, there is no prior literature report of electroluminescence from blends of donor and acceptor conjugated polymers.

Blends of donor and acceptor conjugated polymers with favorable electronic structures (HOMO/LUMO levels) represent one option to achieve balanced charge injection and transport in polymer light-emitting diodes. However, to avoid or minimize photoinduced charge transfer and quenching of electroluminescence in such bipolar blends of conjugated polymers, the blend components should be such that their electronic structures favor excitation energy transfer and disfavor electron transfer. Because the conjugated polyquinolines have

10.1021/ma0346299 CCC: $25.00
Published on Web 07/24/2003

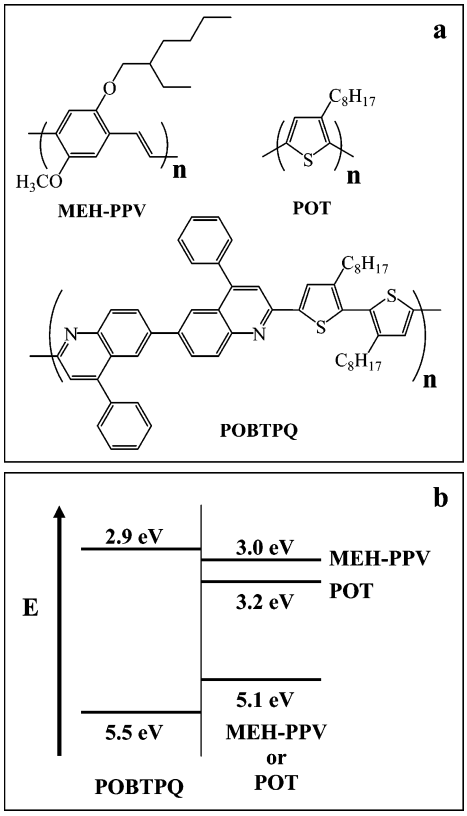

Figure 1. (a) Chemical structures and (b) HOMO/LUMO energy level diagram of conjugated polymers POBTPQ, MEH−PPV, and POT.

documented n-type (electron accepting) properties,[15] we selected the organic-solvent-soluble poly(2,2′-(3,3′-dioctyl-2,2′-bithienylene)-6,6′-bis(4-phenylenequinoline)) (POBTPQ)[15d] as an n-type conjugated polymer blend component. In this paper, we report the morphology, photophysics, electroluminescence (EL), and LED performance of binary blends of POBTPQ as the electron transport (n-type) component[15d] and poly(2-methoxy-5(2′-ethyl-hexyloxy)-1,4-phenylenevinylene) (MEH−PPV) or poly(3-octylthiophene) (POT) as a hole transport (p-type) component.[2,3h] The molecular structures and the HOMO/LUMO energy level diagram[16] of these polymer blend components are given in Figure 1. The phase-separated morphology of the blends was investigated as a function of composition by atomic force microscopy (AFM). The photophysical properties and electroluminescence from blend LEDs were also investigated as a function of blend composition. Efficient electroluminescence was achieved in both binary donor−acceptor blend systems, and voltage-tunable multicolor LEDs were observed in the POBTPQ:MEH−PPV blend system.

Experimental Section

Materials. The POBTPQ sample used in this study was recently synthesized in our laboratory. The synthesis, characterization, electrochemistry, thin film processing, optical, and electroluminescent properties of POBTPQ ($M_w \sim 64\,900$) have been reported elsewhere.[15d] MEH−PPV ($M_w \sim 85\,000$) was purchased from American Dye Source, Inc., and POT ($M_w \sim 39\,200$) and poly(ethylenedioxythiophene)/poly(styrenesulfonic acid) (PEDOT; solution in water) were obtained from Aldrich.

Preparation of Blends and Thin Films. Binary blends of POBTPQ and MEH−PPV (or POT) were prepared by dissolving them with appropriate weight percent ratio in chloroform in which all three polymers are very soluble. The resulting blend solutions were homogeneous. Compositions of blends in this paper refer to weight percentage of MEH−PPV (or POT). A series of blend compositions including 1, 3, 5, 10, 20, 30, 40, 50, 70, 77, 84, and 91 wt % MEH−PPV (or POT) were prepared. All thin films of the homopolymers or binary blends investigated in this study were obtained by spin-coating from their $CHCl_3$ solutions. The thin films used for optical absorption and photoluminescence measurements were spin-coated onto silica substrates. All the films were dried in a vacuum at 60 °C for 8 h to remove any trace of residual solvent. The thin films of binary blends were homogeneous and showed excellent optical transparency. No visible phase separation was observed.

Photophysics and Surface Morphology. Optical absorption spectra were obtained by using a Lambda-900 UV/vis/near-IR spectrophotometer (Perkin-Elmer). Photoluminescence (PL) studies were carried out on a Spex Fluolog-2 spectrofluorimeter. The thin films were positioned such that the emitted light was detected at 22.5° from the incident beam.[9,12a,b,d] For morphological investigations, the thin films of polymer blends (POBTPQ:MEH−PPV and POBTPQ:POT) were spin-coated from their blend solutions in $CHCl_3$ onto polished silicon substrates and dried at 60 °C in a vacuum for 12 h. Atomic force microscopy (AFM) images were obtained using a Nano-Scope III microscope (Digital Instruments Inc., Veeco Metrology group, Santa Barbara, CA) in standard tapping mode with single silicon-crystal tip as nanoprobe.

Fabrication and Characterization of LEDs. Electroluminescent devices were fabricated and investigated as sandwich structures between two electrodes where aluminum (Al) was used as cathode and indium−tin oxide (ITO) was used as anode.[3f−h,9] The thin films of homopolymers or their binary blends were spin-coated from their 0.5 wt % solution in $CHCl_3$ onto precleaned ITO-coated glass substrates (Delta Technologies, Ltd., Stillwater, MN; $R_s = 8-12\ \Omega/\square$) and dried at 60 °C in a vacuum for 8 h.[3h,9,15d] In some devices, a thin layer of poly(ethylenedioxythiophene)/poly(styrenesulfonate) (PEDOT) (<40 nm) was first spin-coated from its solution in water onto ITO substrates and dried at 80 °C in a vacuum for 10 h. Then, the homopolymer or blend layer was spin-coated onto the PEDOT layer and dried in a vacuum at 60 °C for 8 h. The film thicknesses were measured by an Alpha-step profilometer (model 500, KLA Tencor, San Jose, CA) with an accuracy of ±1 nm and confirmed by an optical absorption coefficient technique. Finally, a 100−120 nm thick aluminum layer was thermally deposited under high vacuum ($\sim 3 \times 10^{-6}$ Torr) onto the polymer or blend layer to form an active diode area of 0.2 cm^2 (5 mm diameter). Electroluminescence (EL) spectra were measured on a SPEX Fluorolog-2 spectrofluorimeter. Electroluminescence microscopy of the LEDs was done by using a Leica fluorescence microscope. The true color images of light emitted from the LEDs under applied bias voltages was captured by a Hamamatsu Orca II CCD camera (C4742-98) using Openlab 2.2.5 imaging software in a PC. Current−voltage ($I-V$) and luminance−voltage ($L-V$) curves were recorded simultaneously by hooking up an HP4155A semiconductor parameter analyzer (Yokogawa Hewlett-Packard, Tokyo) together with a Grasby S370 optometer (Grasby Optronics, Orlando, FL) equipped with a calibrated luminance sensor head (model 211).[3f−h,9,15d] The EL quantum efficiencies of the diodes were measured by using procedures similar to that previously reported.[3f−h,9,15d] All the fabrication and measurements were done under ambient laboratory conditions.

Electric-Field-Induced Photoluminescence Spectroscopy. Electric-field-induced PL measurements were performed on the same electroluminescent devices described above after their EL properties were characterized.[9] An LED sample was photoexcited, and the PL emission spectrum was acquired under an applied bias voltage. Both forward (positive to ITO) and reverse bias voltages gave identical PL spectra before EL emission. The device was positioned in such a way that the emitted light was detected from the ITO side at 22.5° relative to the incident beam. All the experiment conditions were the same as in the steady-state PL measurements on thin films on silica substrates.

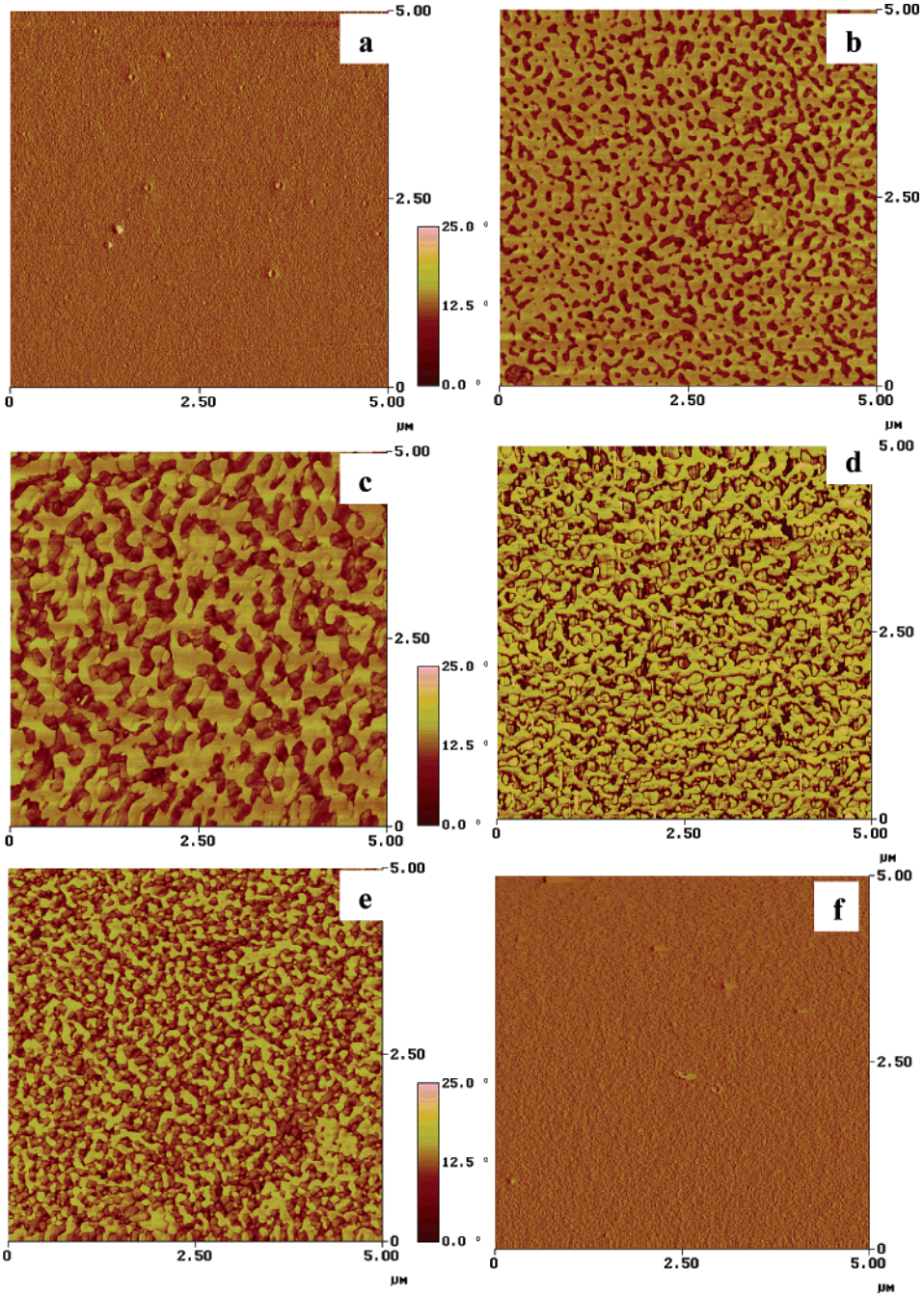

Figure 2. Tapping-mode AFM phase images of POBTPQ, MEH−PPV, and their blend thin films on silicon substrates spin-coated from chloroform solution: (a) POBTPQ, (b) 20 wt %, (c) 40 wt %, (d) 50 wt %, (e) 70 wt % MEH−PPV, and (f) MEH−PPV.

Results and Discussion

Morphology of Binary Blends. The 5 μm × 5 μm AFM phase images of the surface morphology of POBTPQ:MEH−PPV blend thin films on silicon substrates as a function of composition are shown in Figure 2. The AFM phase images of both POBTPQ and MEH−PPV homopolymers, shown in parts a and f of Figure 2, respectively, were smooth and featureless. Two distinct phases were observed in the morphology of the blends. The dark features in Figure 2b−e increase with increasing wt % of MEH−PPV, suggesting that the dark regions represent the MEH−PPV phase and the light regions represent the POBTPQ phase. The phase separation length scale ranges from 90 to 120 nm. The nanophase-separated morphology observed in these blends is characteristic of dimixing via spinodal decomposition.[17] At a higher concentration of MEH−PPV (~84 wt % or higher) in the binary blends, the absence of identifiable two phases and appearance of a highly oriented morphology were observed (Figure 3). The feature width of the oriented domains was 100−120 nm. We note that the same directional orientation in the blend morphology seen in Figure 3 was also observed by changing the direction of tip scan 90° to the original scan. This rule out AFM tip-induced alignment as the origin of the oriented morphology in these high MEH−PPV-containing blends.

The AFM phase image of poly(3-octylthiophene) (POT) homopolymer was also smooth and featureless (not shown). Two different phases were observed in the surface morphology of POBTPQ:POT blends as shown in the representative topographical AFM images of

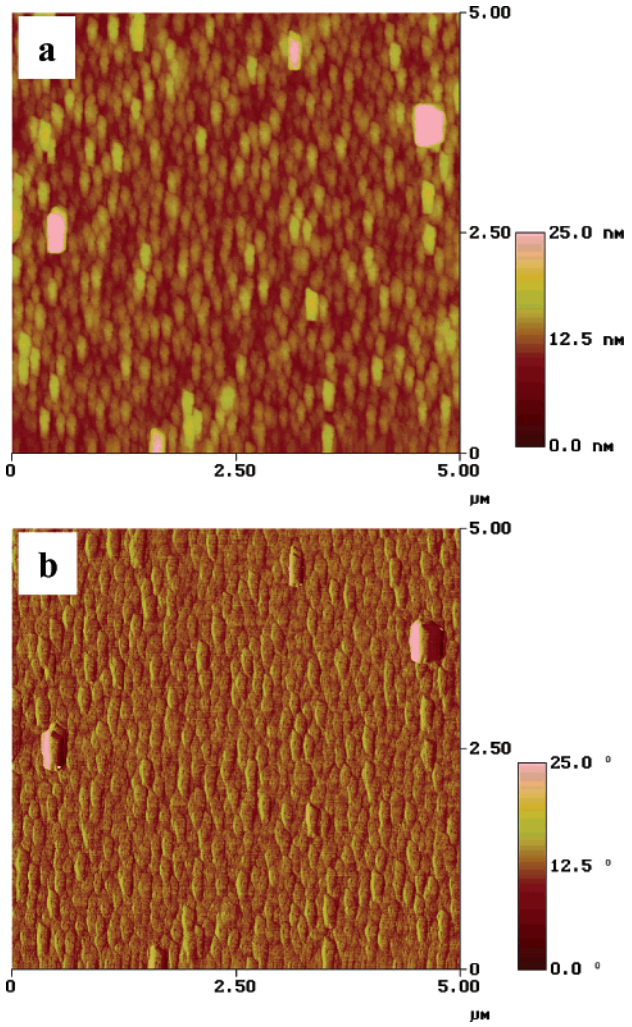

Figure 3. (a) Topographical and (b) phase AFM images of 84 wt % MEH−PPV blend thin film on silicon substrates spin-coated from chloroform solution.

Figure 4. In this case, the nanophase-separated morphology is characteristic of dimixing through the nucleation and growth mechanism.[17] The domain sizes of the phase-separated morphology of this binary blend system increased with increasing POT composition, suggesting that the circular dark regions represent the POT phase. The domain size of the spherical POT phase varied from 50 nm at 5 wt % to 400 nm at 30 wt % POT. At lower wt % POT (≤10%) in these blends, the AFM images showed a uniform distribution of POT domains in the POBTPQ matrix from which an enhanced device performance can be expected because of the higher surface area for interaction between POT and POBTPQ.

Photophysical Properties. Optical absorption and photoluminescence (PL) spectra of thin films of POBTPQ and MEH−PPV are shown in Figure 5a. POBTPQ has an absorption peak at 414 nm and a PL emission peak at 530 nm.[15d] The PL spectrum of POBTPQ and the absorption spectrum of MEH−PPV overlap to a reasonable extent in the 450−600 nm regions from which Förster-type (dipole−dipole interactions) energy transfer from POBTPQ to MEH−PPV can be expected. Similar Förster energy transfer from POBTPQ to POT can be expected due to their absorption and PL spectral overlap in the 460−660 nm region (Figure 5b). Figure 6a shows the absorption spectra of thin films of POBTPQ:MEH−PPV binary blends with peaks at 414 nm

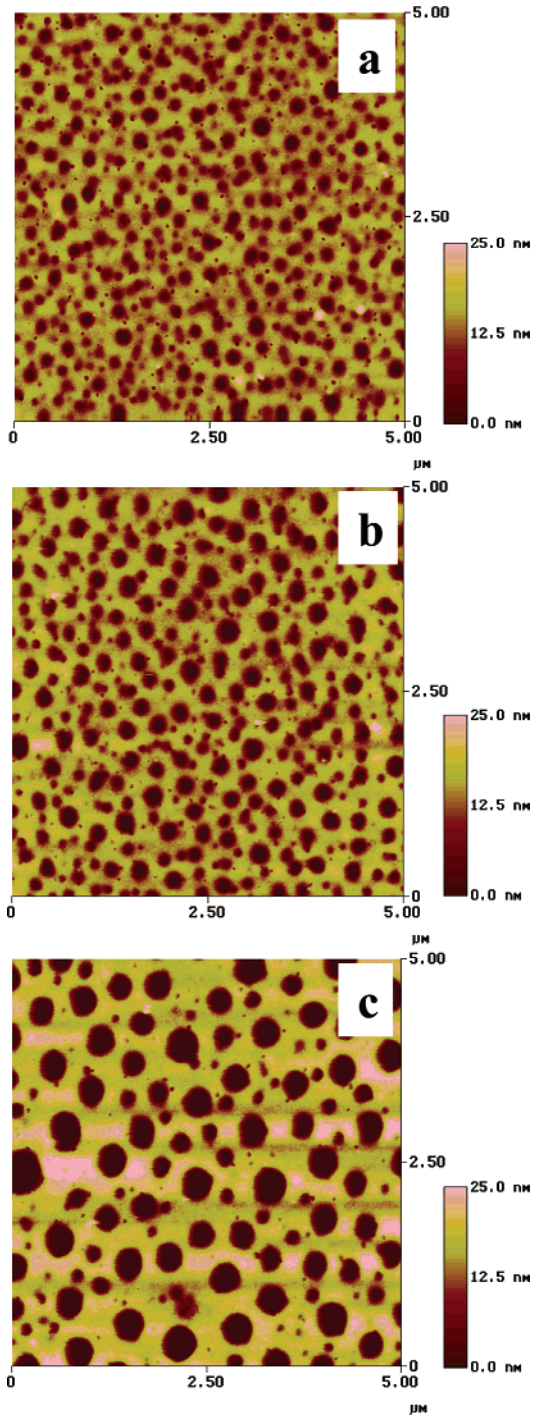

Figure 4. Topographical AFM images of POBTPQ:POT blend thin films on silicon substrates spin-coated from chloroform solution: (a) 5 wt %, (b) 10 wt %, and (c) 30 wt % POT blends.

due to POBTPQ and 500 nm due to MEH−PPV. The absorption spectra of the blends are simple superpositions of those of the component POBTPQ and MEH−PPV homopolymers. No new absorption features were observed in the wavelength range of 200−2000 nm, suggesting that the two blend components have no observable interactions in their electronic ground states. Similar results were observed in POBTPQ:POT blends.

The thin film PL emission spectra of POBTPQ:MEH−PPV blends (414 nm excitation) are shown in Figure 6b. The POBTPQ and MEH−PPV homopolymers showed PL emission maxima at 530 and 585 nm, respectively. In the binary blends, only an orange-red PL emission

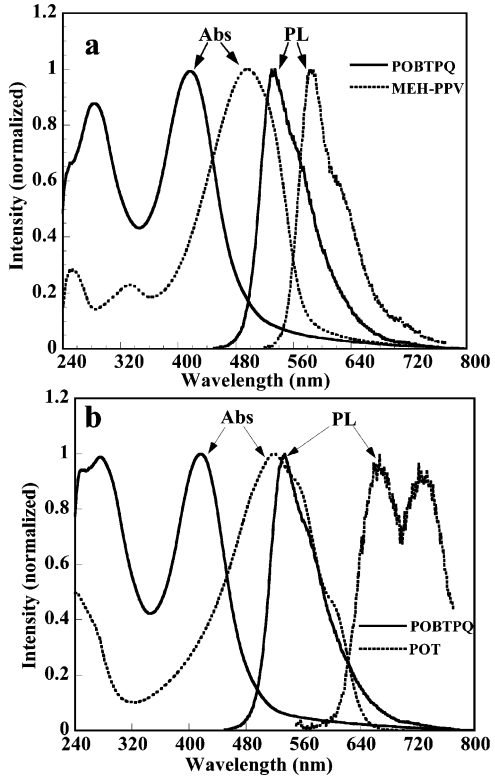

Figure 5. Normalized optical absorption and PL spectra of thin films on silica substrates: (a) POBTPQ and MEH−PPV; (b) POBTPQ and POT.

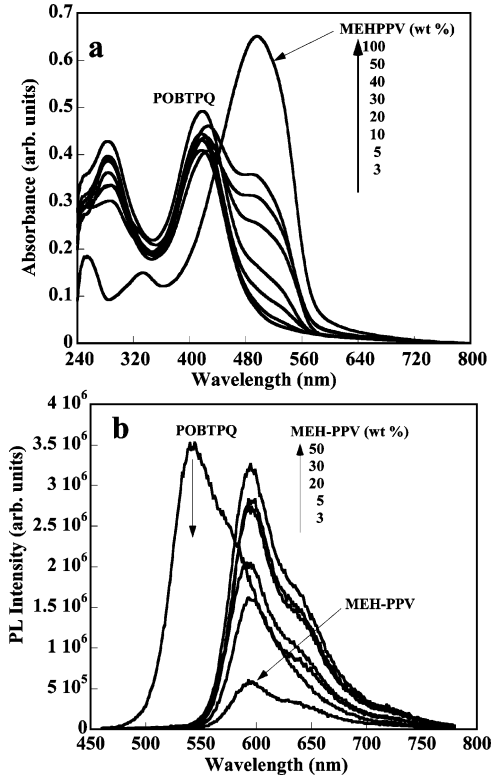

Figure 6. (a) Optical absorption and (b) PL spectra of thin films of POBTPQ, MEH−PPV, and their blends on silica substrates. The excitation wavelength was 414 nm for all spectra.

band at 585 nm, which is characteristic of MEH−PPV emission,[3h] was observed. The PL intensity of this 585 nm emission band in the blends is significantly enhanced compared to that of the pure MEH−PPV. The intensity of this PL emission band at 585 nm increased with increasing concentration of MEH−PPV in the blends, saturating at around 50 wt % MEH−PPV. These observations suggest efficient Förster energy transfer from the excited state of POBTPQ to MEH−PPV, as expected. The energy-transfer efficiency (χ) was calculated by using the relation[18a,b]

$$\chi = \frac{\phi_D}{\phi_D + \phi_A(I_D/I_A)}$$

where I_A and I_D are the integrated PL intensities of the energy acceptor and donor, respectively, with a constant excitation wavelength of 414 nm for all the blends and homopolymers; ϕ_A and ϕ_D are respectively the PL quantum efficiencies of the energy acceptor and donor. From the known PL quantum efficiencies of 4% for POBTPQ[15d] and 15% for MEH−PPV,[19] the energy-transfer efficiency was estimated to be 23% at 3 wt % MEH−PPV to a maximum of 58% at 50 wt % MEH−PPV. Similar efficient Förster energy transfer from the excited state of POBTPQ to the red-emitting POT (emission maximum around 660 nm) was observed. In this case the maximum energy-transfer efficiency was found to be 66% at 10 wt % POT (ϕ_A = 2%)[19] in the POBTPQ:POT blends. These observations of highly efficient excitation energy transfer among components of binary blends of donor and acceptor conjugated polymers contrast sharply with such prior blends in which either photoinduced[4,11] or ground-state[10] charge transfer was observed. These results thus highlight the important role of the electronic structures (HOMO/LUMO levels) of the components in the *supramolecular properties* of blends of conjugated polymer semiconductors.

The extent of the Förster energy transfer between POBTPQ (energy donor) and MEH−PPV (or POT) (energy acceptor) can be evaluated via the Förster radius, R_0, from the following equation:[18]

$$R_0^6 = \frac{9000 \ln 10 \kappa^2 \phi_D}{128 \pi^6 n^4 N_A} \int_0^\infty f_d(\nu)\, \epsilon_a(\nu)\, \frac{d(\nu)}{\nu^4}$$

where ν is the wavenumber, ϵ_a is the molar extinction coefficient of the energy acceptor, f_d is the normalized PL spectral distribution of the excitation donor, ϕ_D is the PL quantum yield of the energy donor, N_A is Avogadro's number, n is the refractive index of the blend, and κ^2 is an orientation factor, which in the case of random directional distribution is $^2/_3$. From the normalized PL spectrum of POBTPQ and molar extinction coefficient of MEH−PPV (or POT) thin films, we obtained the values of spectral overlap integral $\{J = \int_0^\infty f_d(\nu)\epsilon_a(\nu)/\nu^4\, d(\nu)\}$ to be 2.09×10^{-11} cm^3 for POBTPQ:MEH−PPV blends and 2.33×10^{-11} cm^3 for POBTPQ:POT blends. Assuming n = 1.6 for the blends, the Förster radius, R_0, was estimated to be 5.1 nm for POBTPQ:MEH−PPV blends and 5.5 nm for POBTPQ:POT blends. The larger Förster radius (5.5 nm) and the higher degree of spectral overlap confirm the observed higher energy-transfer efficiency in POBTPQ:POT blends compared to that in POBTPQ:MEH−PPV blends.

Electroluminescence from Binary Blends. Green electroluminescence (EL) was observed from POBTPQ diodes of the type ITO/PEDOT/POBTPQ/Al at forward bias voltages, and the EL spectrum was identical to its

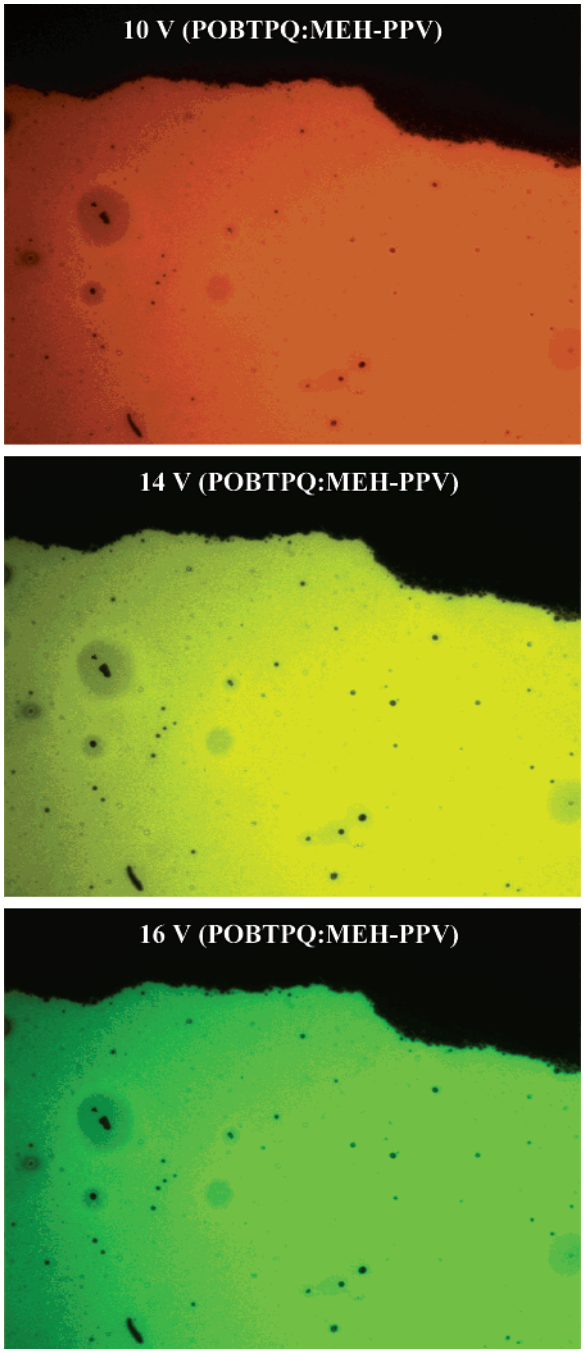

Figure 7. EL micrographs (×10) of a POBTPQ:MEH−PPV (30:70 wt %) blend LED.

PL spectrum.[15d] The EL devices made from POBTPQ:MEH−PPV blends showed reversible color change from green to yellow to orange-red under a varying bias voltage. Such EL devices, ITO/PEDOT/blend/Al, emitted bright orange-red color at low bias voltages (9−12 V) and yellow to green colors at higher forward bias voltages. EL micrographs of a typical color-tunable POBTPQ:MEH−PPV blend (30:70 wt %) diode under different bias voltages are shown in Figure 7. The dark spots seen in the EL micrographs are very similar to those previously observed in organic LEDs and are nonemissive areas due to fabrication defects.[3g] The size and distribution of the dark spots in these blend diodes do not grow with increasing voltage or time. This suggests that the dark spots seen here are preexisting defects associated with the device fabrication and are not evidence of EL diode degradation sites.

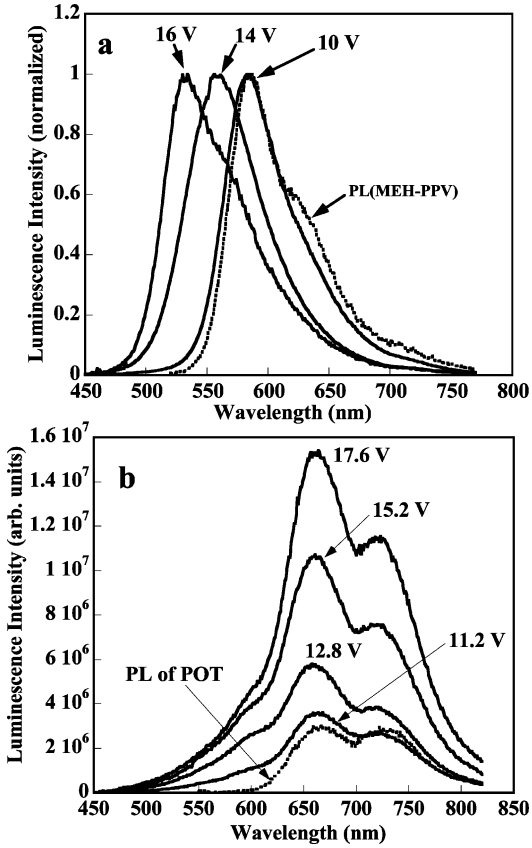

Figure 8. (a) Voltage-tunable EL spectra of 70 wt % MEH−PPV blend diodes with the PL spectrum of MEH−PPV thin film. (b) EL spectra of 10 wt % POT blend diodes at different forward bias voltages with the PL spectrum of POT thin film.

The bias voltage-tunable EL spectra corresponding to the EL micrographs of Figure 7 are shown in Figure 8a. The orange-red EL emission (λ_{max} = 585 nm) observed at low bias voltages is identical with that of the single-layer MEH−PPV diodes, showing that the orange-red EL emission came from the MEH−PPV component in the blend. The observed green EL emission at higher bias voltages (>15 V) is identical with that of the single-layer POBTPQ diodes, which means that excitons are created by the recombination of charges in the POBTPQ domains and emits its characteristic green EL color in the blend. The yellow EL emission observed at an intermediate bias voltage in the blend LEDs is a result of simultaneous emission of green and orange-red colors from both blend components, leading to the observed yellow color. Similar voltage-tunable LED colors have previously been observed in bilayered thin films.[3c,g] Voltage-tunable multicolor EL emission was observed in the blend LEDs for all compositions up to 80 wt % MEH−PPV. At a higher concentration of MEH−PPV (>80%), only the orange-red EL emission from MEH−PPV was observed. This blend composition coincides with that from AFM studies which showed that above this composition (~80−84 wt %) only a single phase with oriented morphology existed. This implies that a nanophase-separated morphology is essential to achieve the voltage-tunable multicolor emission from blend LEDs.

The observed voltage-tunable multicolor EL emission from the POBTPQ:MEH−PPV blend LEDs means that both charge transfer and energy transfer across the nanophase-separated boundaries are important. On the basis of the previously discussed PL studies, we ex-

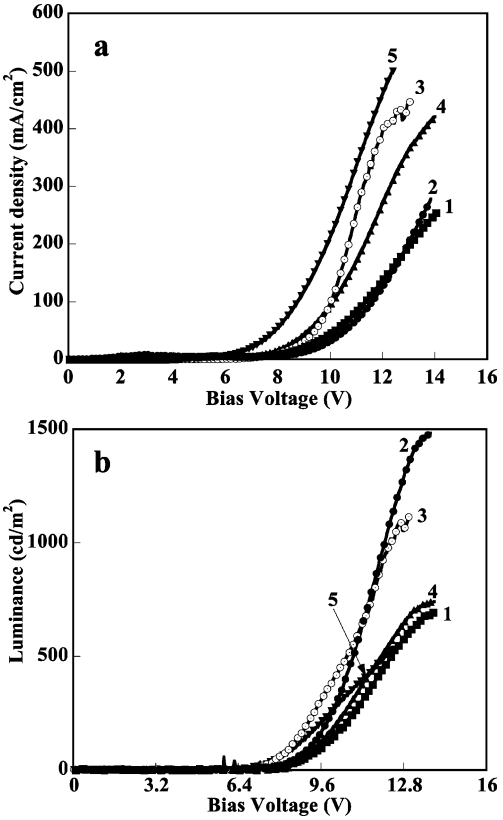

Figure 9. (a) Current−voltage and (b) luminance−voltage curves of POBTPQ:MEH−PPV blend LEDs made from (1) 50 wt %, (2) 70 wt %, (3) 77 wt %, (4) 84 wt %, and (5) 91 wt % MEH−PPV.

pected only orange EL emission from the MEH−PPV phase because of efficient energy transfer from the POBTPQ phase. However, in the EL devices electron and hole transfer across phase boundaries occur at different rates, resulting in recombination and exciton generation rates that are different in the two domains of the blends. Furthermore, exciton generation rate in the POBTPQ domain clearly exceeds the rate of energy transfer from POBTPQ to MEH−PPV, leading to simultaneous emission from both domains of the blend LEDs. It is the electric field dependent dynamics of energy- and charge-transfer processes in the POBTPQ:MEH−PPV blend system that manifest as the observed voltage-tunable LED colors.

In the case of POBTPQ:POT blend LEDs, only red EL emission (λ_{max} = 660 nm) was observed at all forward bias voltages (Figure 8b). These EL spectra are identical with that of the single-layer ITO/POT/Al diodes and the PL emission of POT. These results show that excitons are created in the POT domains in the blends by the efficient Förster energy transfer from POBTPQ to POT, as observed above in the PL spectroscopy. Although some direct charge recombination within the POT domains cannot be completely ruled out, contribution from this to the EL emission is likely to be negligibly small. For example, no EL emission was observed at higher concentrations of POT (>50%) in the blends. At these very high concentrations of POT, the domains of POT in the blend were rather large (>400 nm), as previously discussed above under morphology.

Figure 9 shows representative current−voltage and luminance−voltage curves of the blend LEDs, ITO/PEDOT/Blend/Al, made from the POBTPQ:MEH−PPV blend system. LEDs made from either POBTPQ or MEH−PPV homopolymer, ITO/PEDOT/polymer/Al, had poor device performance. The turn-on voltage and maximum brightness of the blend LEDs are collected in Table 1. The 70 wt % MEH−PPV blend diode showed bright EL emission with a turn-on voltage of 5.5 V and a luminance of 1490 cd/m^2 at 14 V. From the 77 wt % MEH−PPV blend diode, similar bright EL emission was observed with a luminance of 1115 cd/m^2 at 13 V. The turn-on voltage of the blend LEDs decreased with increasing wt % MEH−PPV, reaching a 5.5 V saturation at around 40−50 wt %. The blend devices containing 40−91 wt % MEH−PPV have the lowest turn-on voltage of 5.5 V, which is much lower than that of the single-layer POBTPQ diode and is comparable with the turn-on voltage of the single-layer MEH−PPV diode. The luminance of the blend LEDs was substantially enhanced compared to that of the single-layer MEH−PPV or POBTPQ diode. The luminance values of the 70 and 77 wt % MEH−PPV blend LEDs are factors of 7−28 times greater than that of the single-layer MEH−PPV or POBTPQ diode. Enhancement of device luminance was also observed for LEDs from other blend compositions (Table 1). These results suggest improved charge injection and recombination in the bipolar blend diodes compared to the component homopolymer single-layer diodes.

Table 1. Performance of Blend LEDs: ITO/PEDOT/POBTPQ:MEH−PPV/Al

composition, wt % MEH−PPV	V_{on}, V	J_{max}, mA/cm^2	L_{max}, cd/m^2	V_{max}, V	Φ_{ext}, %
0	9	53	53	17.5	0.06
1	11	146	42	20	0.013
3	11	137	57	20	0.019
5	11	148	120	20	0.037
10	8.5	162	202	20	0.073
20	6	192	339	20	0.15
30	6	163	484	15.6	0.35
40	5.5	146	592	14	0.44
50	5.5	254	703	14	0.53
70	5.5	279	1490	14	0.70
77	5.5	447	1115	13	0.35
84	5.5	421	743	14	0.21
91	5.5	500	543	12	0.15
100	4	238	228	7	0.30

The composition-dependent performance data of the blend LEDs, including the composition, turn-on voltage (V_{on}), maximum luminance (L_{max}) with the corresponding operating voltage (V_{max}), current density (J_{max}), and external quantum efficiency (Φ_{ext}), are summarized in Table 1 for the POBTPQ:MEH−PPV blend system. The external quantum efficiencies (photons/electron) of the single-layer POBTPQ and MEH−PPV homopolymer diodes were 0.06 and 0.3%, respectively. The external quantum efficiency of the blend devices varied from 0.004 to 0.70% depending on the blend composition. The 50 and 70 wt % blend diodes had the highest external quantum efficiencies of 0.53 and 0.70%, respectively. This represents a factor of 2−12 enhancement compared to that of the component single-layer homopolymer LEDs. Blending of n-type POBTPQ with p-type MEH−PPV has thus resulted in a large enhancement in the bipolar blend LED performance.

The performance of blend LEDs of the type ITO/POBTPQ:MEH−PPV/Al was also investigated. The external quantum efficiency of the reference ITO/MEH−PPV/Al diode was 0.02% with a maximum light output of 163 cd/m^2 at 15.5 V and a turn-on voltage of 12 V (Table 2). The ITO/POBTPQ/Al diode did not emit light

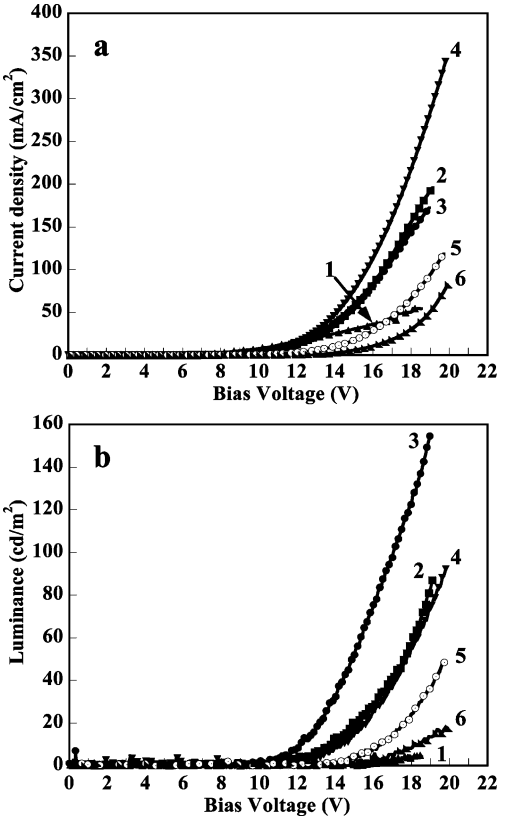

Figure 10. (a) Current−voltage and (b) luminance−voltage curves of POBTPQ:POT blend LEDs made from (1) 1 wt %, (2) 5 wt %, (3) 10 wt %, (4) 20 wt %, (5) 30 wt %, and (6) 40 wt % POT.

Table 2. Performance of Blend LEDs: ITO/POBTPQ:MEH−PPV/Al

composition, wt % MEH−PPV	$V_{on,}$ V	J_{max}, mA/cm^2	L_{max}, cd/m^2	V_{max}, V	Φ_{ext}, %
0					
1	14	500	88	18	0.003
3	13	500	120	19	0.004
5	12	500	143	17	0.014
10	10	500	193	20	0.019
20	9.5	480	209	20	0.022
30	9.5	460	222	15	0.038
40	9	469	229	13	0.043
50	8.5	463	237	12	0.05
70	8.5	429	272	15	0.09
77	8	190	416	14.5	0.20
84	7.5	263	318	14	0.11
91	7.5	234	310	16	0.10
100	12	500	163	15.5	0.02

even at higher operating voltages (>20 V). As shown in Table 2, all the POBTPQ:MEH−PPV blend LEDs have enhanced performance compared to that of the single-layer POBTPQ, and most of the blend LEDs were superior to the MEH−PPV device. The 77 wt % MEH−PPV blend diode showed the best performance with an external quantum efficiency of 0.2% and a maximum brightness of 416 cd/m^2 at 14.5 V and a turn-on voltage of 8 V. The turn-on voltage of the blend LEDs was in the range 7.5−14 V, and it decreased with increasing MEH−PPV content. This is consistent with the results for blend LEDs incorporating a PEDOT hole injection layer.

The current−voltage and the luminance−voltage curves of LEDs fabricated from bipolar POBTPQ:POT blends, ITO/PEDOT/blend/Al, are shown in Figure 10. The current through the devices showed characteristic

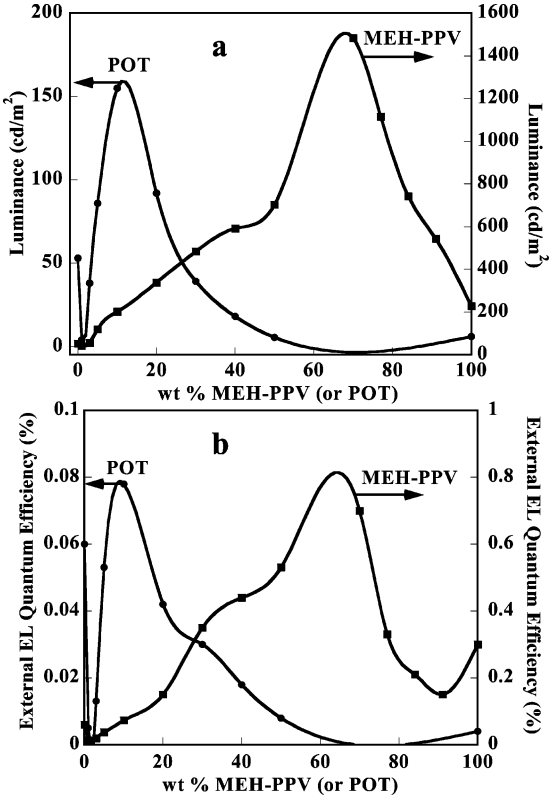

Figure 11. (a) Luminance and (b) external EL quantum efficiency as a function of blend composition.

Table 3. Performance of Blend LEDs: ITO/PEDOT/POBTPQ:POT/Al

composition, wt % POT	V_{on}, V	J_{max}, mA/cm^2	L_{max}, cd/m^2	V_{max}, V	Φ_{ext}, %
0	9	53	53	17.5	0.06
1	15	55	4	18.5	0.005
3	10	169	38	17	0.013
5	10	196	86	19	0.053
10	9	172	155	19	0.08
20	10	343	92	20	0.042
30	13	119	49	20	0.03
40	14	82	18	20	0.018
50	14	202	6	20	0.008
100	4	500	6	7.5	0.003

Table 4. Performance of Blend LEDs: ITO/POBTPQ:POT/Al

composition, wt % POT	V_{on}, V	J_{max}, mA/cm^2	L_{max}, cd/m^2	V_{max}, V	Φ_{ext}, %
0					
1	15	377	8	20	0.002
3	10	293	24	16	0.008
5	7	179	59	12	0.023
10	6.5	238	116	10	0.075
20	10	232	67	20	0.015
30	12	197	33	20	0.007
40	16	130	11	20	0.003
50					
100	11	500	3	19	0.0003

diode field dependence. Bright red EL emission with a turn-on voltage of 9 V and a luminance of 155 cd/m^2 at 19 V was observed for the 10 wt % POT blend diodes (Table 3). A turn-on voltage of 10 V and a luminance of 92 cd/m^2 (at 20 V) were observed for the 20 wt % POT blend LEDs. The external quantum efficiency of the single component POT diode was only 0.003%, whereas those of the best POBTPQ:POT blend diodes were 0.053−0.08%. The external quantum efficiency is thus

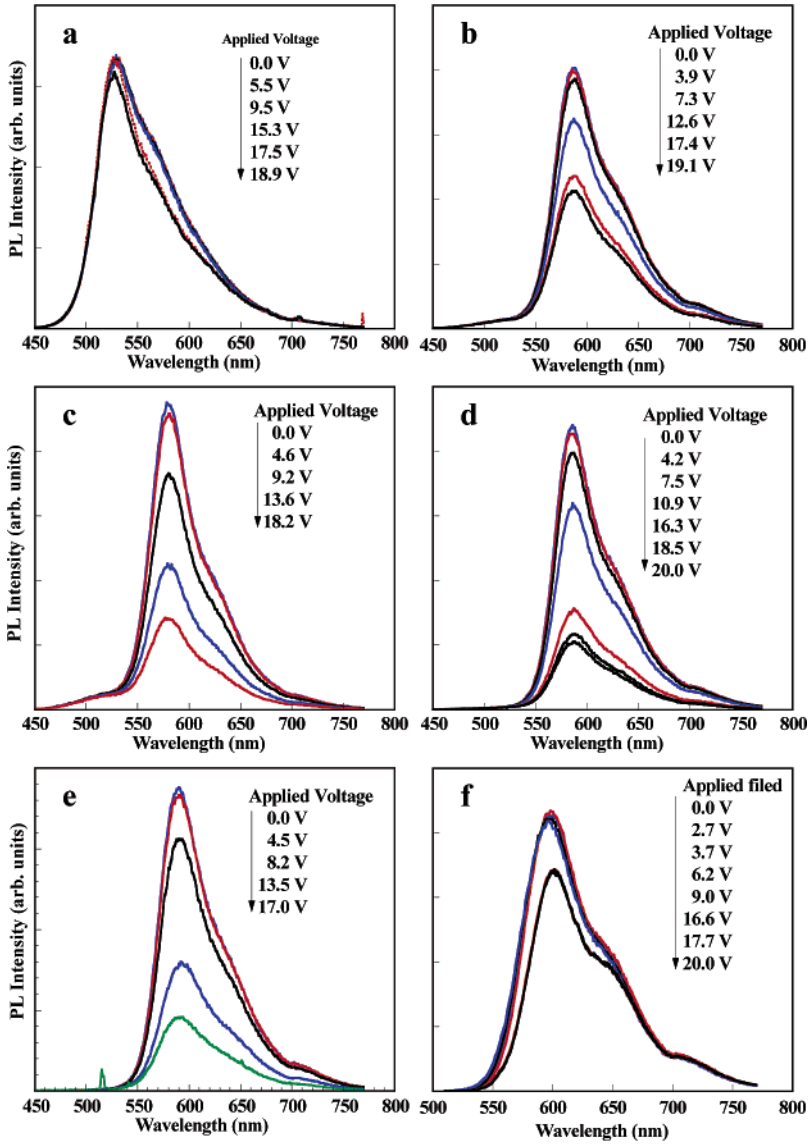

Figure 12. Electric-field-modulated PL spectra of POBTPQ, MEH−PPV, and their blends at various reverse bias voltages: (a) POBTPQ, (b) 30 wt %, (c) 50 wt %, (d) 70 wt %, (e) 91 wt % MEH−PPV, and (f) MEH−PPV.

enhanced by a factor of 18−27 times compared to those of the POT homopolymer diodes. Improvement in performance of the blend LEDs with other POT concentrations was also observed (Table 3). Overall smaller enhancement in LED performance was observed in blend devices without the PEDOT hole injection layer, ITO/POBTPQ:POT/Al (Table 4). The external quantum efficiency of the ITO/POT/Al diode was 0.0003%, whereas the blend devices with 10 wt % POT content had an external quantum efficiency of 0.075%. This is a factor of 250 greater than that of the POT homopolymer diodes. The enhanced performance of these bipolar blend LEDs implies improved charge (both hole and electron) injection and recombination compared to the case of single component diodes.

The composition dependencies of the luminance and external EL quantum efficiency of the blend LEDs are shown in parts a and b of Figure 11, respectively. One of the striking features of these results is the sharp difference between the MEH−PPV and POT blend systems even though they both contain POBTPQ. In the case of the POBTPQ:MEH−PPV blend system, enhancement in the LED performance increases with composition until a peak at about 70 wt % MEH−PPV. In contrast, the POBTPQ:POT blend system shows enhancement in LED performance over a narrow composition region with a peak at 10 wt % POT. One obvious reason for this difference in composition-dependent blend LED performance between the two POBTPQ blend systems is the vast difference in the phase-separated morphology. The nucleation and growth morphology in which spherical POT particles are dispersed in POBTPQ matrix (Figure 4) is most favorable to energy transfer and bipolar charge transport in the less than 40 wt % POT blend composition region. The similarity of the domain size and spinodal decomposition morphology of the MEH−PPV blend up to ca. 80 wt % (Figures 2 and 3) accounts for the enhancement in LED performance over the broad blend compositions up to 80 wt %. This morphology is ideal for efficient energy transfer and for bipolar charge transport as confirmed by the voltage-dependent multicolor emission from the blend LEDs (Figures 7 and 8a). The rapid decrease in enhancement in LED performance at the very high MEH−PPV containing blends can be explained by the change in morphology (at ∼80 wt %) and the reduction in electron transport due to the smaller amount of POBTPQ.

Electric Field-Induced Photoluminescence Quenching in Blends. The beneficial bipolar charge transport in blend LEDs made from donor−acceptor conjugated polymers could in principle also facilitate facile exciton dissociation under the typical high electric fields of devices. Composition-dependent exciton dissociation in the binary blends was therefore investigated by electric-field-modulated photoluminescence (PL) spectroscopy. Electric-field-induced PL quenching due to exciton dissociation in conjugated polymers has been reported by our group and others.[9,14] The PL spectra of POBTPQ, MEH−PPV, and their blend devices under various reverse bias voltages are shown in Figure 12. The measurements under forward bias voltages before the EL device turned on gave identical PL spectra as those under reverse bias voltages, indicating that the electric field only modulates the PL spectra and that there is no contribution from EL emission. To obtain PL spectra under higher electric fields, we applied reverse bias voltages where there is no EL emission.[9,14] The PL intensity drops only about 6% for the POBTPQ homopolymer at 19 V and around 20% for MEH−PPV at 20 V, as shown in parts a and f of Figure 12, respectively. In the POBTPQ:MEH−PPV blends, the PL intensity decreased with increasing concentration of MEH−PPV; almost 75−80% decrease was observed in the composition range of 50−91 wt % MEH−PPV (Figure 12b−e). Similarly, the POT homopolymer shows less than 3% PL quenching, whereas the maximum PL quenching was about 20−30% at 10−20 wt % POT in the POBTPQ:POT blends.

Figure 13 shows the relative PL efficiency of the homopolymers and their blends as a function of applied electric field. The POBTPQ and MEH−PPV homopolymers show 7−20% PL quenching at the highest electric fields (Figure 13a), which indicates that the excitons are relatively stable in the homopolymers. Under the applied electric fields the PL efficiency decreased by up to 75−80% (Figure 13a), suggesting that excitons were dissociated into free charges and transported through the respective n-type or p-type polymer in the POBTPQ:MEH−PPV blends. Similar results were observed in the bipolar POBTPQ:POT blends under the applied electric field, as shown in Figure 13b. These results show that donor−acceptor conjugated polymer blends are more susceptible to electric-field-induced exciton dissociation compared to unipolar blends in which exciton stability was significantly enhanced compared to the homopolymers due to spatial confinement.[9]

The finding that electric-field-induced PL quenching is enhanced in these donor−acceptor conjugated polymer blends is to be expected from their bipolar nature. Effective dissociation of excitons under an electric field requires that both carrier types (electrons and holes) be transported toward opposite electrodes. This requirement is readily met in the bipolar (n-type/p-type) conjugated polymer blends investigated here, POBTPQ:MEH−PPV and POBTPQ:POT. In contrast, in an n-type conjugated polymer such as POBTPQ, electron transport is favorable over hole transport, which can significantly hinder the dissociation of excitons into free charges. Similar stability of excitons in a p-type homopolymer (MEH−PPV or POT) is due to the preferential transport of holes toward the negative electrode under an electric field. Similar considerations apply to *all n-type* or *all p-type* blends of conjugated polymers in which exciton dissociation under electric fields is

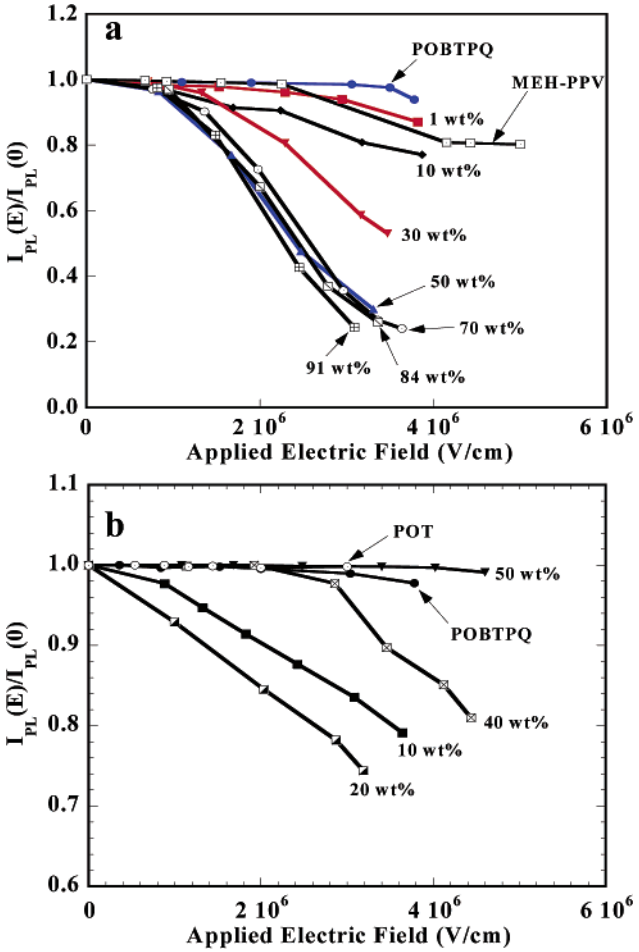

Figure 13. PL quenching as a function of electric field: (a) POBTPQ, MEH−PPV, and their blends; (b) POBTPQ, POT, and their blends. $I_{PL}(0)$ and $I_{PL}(E)$ stand for the integrated PL intensity without and with electric field, respectively.

dramatically retarded.[9] The observed enhancement in performance of bipolar conjugated polymer blend LEDs thus originates from the balanced charge (both electron and hole) injection and transport, leading to improve electron−hole recombination efficiency in the materials. Clearly, however, the achievable luminance and EL external quantum efficiency in bipolar polymer blend LEDs are strong functions of the electronic structures of the blend components.

Conclusions

Binary blends of the n-type conjugated polymer POBTPQ with p-type polymer MEH−PPV or POT were found to be nanophase-separated, bipolar in charge transport, and to exhibit efficient and bright voltage-tunable multicolor electroluminescence. Atomic force microscopy characterization showed that the nanophase-separated POBTPQ:MEH−PPV blends had a spinodal decomposition type morphology with 90−120 nm domains, whereas nucleation and growth type morphology was seen in phase-separated POBTPQ:POT blends. Förster energy transfer, with 5.1−5.5 nm Förster radius, was found to be efficient in both binary blend systems. The finding of efficient electroluminescence from donor−acceptor polymer blend LEDs may at first seems surprising, given that only photoinduced charge transfer and separation,[4,11] leading to complete quenching of electroluminescence,[3g] have previously been seen in donor−acceptor blends. Our results show that ef-

ficient energy transfer rather than charge transfer can occur when the electronic structures (HOMO/LUMO levels) of the donor and acceptor conjugated polymer blend components favor one process over the other. Furthermore, the achievable LED performance can be tuned or optimized by judicious selection of the blend components.

Acknowledgment. This research was supported by the Army Research Office TOPS MURI (Grant DAAD19-01-1-0676) and in part by the Office of Naval Research.

References and Notes

(1) (a) Heeger, A. J. *Angew. Chem., Int. Ed.* **2001**, *40*, 2591. (b) MacDiarmid, A. G. *Angew. Chem., Int. Ed.* **2001**, *40*, 2581.

(2) (a) Friend, R. H.; Gymer, R. W.; Holmes, A. B.; Burroughes, J. H.; Marks, R. N.; Taliani, C.; Bradley, D. D. C.; Dos Santos, D. A.; Bredas, J. L.; Logdlund, M.; Salaneck, W. R. *Nature (London)* **1999**, *397*, 121. (b) Bernius, M. T.; Inbasekaran, M.; O'Brien, J.; Wu, W. *Adv. Mater.* **2000**, *12*, 1737. (c) Kraft, A.; Grimsdale, A. C.; Holmes, A. B. *Angew. Chem., Int. Ed.* **1998**, *37*, 402.

(3) (a) Sokolik, I.; Yang, Z.; Karasz, F. E.; Morton, D. C. *J. Appl. Phys.* **1993**, *74*, 3584. (b) Peng, Z.; Bao, Z.; Galvin, M. E. *Chem. Mater.* **1998**, *10*, 2086. (c) Jenekhe, S. A.; Zhang, X.; Chen, X. L.; Choong, V.-E.; Gao, Y.; Hsieh, B. R. *Chem. Mater.* **1997**, *9*, 409. (d) Tarkka, R. M.; Zhang, X.; Jenekhe, S. A. *J. Am. Chem. Soc.* **1996**, *118*, 9438. (e) Zhang, X.; Shetty, A. S.; Jenekhe, S. A. *Acta Polym.* **1998**, *49*, 52. (f) Zhang, X.; Shetty, A. S.; Jenekhe, S. A. *Macromolecules* **1999**, *32*, 7422. (g) Zhang, X.; Jenekhe, S. A. *Macromolecules* **2000**, *33*, 2069. (h) Alam, M. M.; Jenekhe, S. A. *Chem. Mater.* **2002**, *14*, 4775.

(4) (a) Yu. G.; Heeger, A. J. *J. Appl. Phys.* **1995**, *78*, 4510. (b) Halls, J. J. M.; Walsh, C. A.; Greenham, N. C.; Marseglia, E. A.; Friend, R. H.; Moratti, S. C.; Holmes, A. B. *Nature (London)* **1995**, *376*, 498. (c) Arias, A. C.; MacKenzie, J. D.; Stevenson, R.; Halls, J. J. M.; Inbasekaran, M.; Woo, E. P.; Richards, D.; Friend, R. H. *Macromolecules* **2001**, *34*, 6005.

(5) (a) Antoniadis, H.; Hsieh, B. R.; Abkowitz, M. A.; Jenekhe, S. A.; Stolka, M. *Synth. Met.* **1994**, *62*, 265. (b) Jenekhe, S. A.; Yi, S. *Appl. Phys. Lett.* **2000**, *77*, 2635.

(6) (a) Bao, Z.; Dodabalapur, A.; Lovinger, A. J. *Appl. Phys. Lett.* **1996**, *69*, 4108. (b) Sirringhaus, H.; Tessler, N.; Friend, R. H. *Science* **1998**, *280*, 1741.

(7) (a) Babel, A.; Jenekhe, S. A. *Adv. Mater.* **2002**, *14*, 371. (b) Babel, A.; Jenekhe, S. A. *J. Phys. Chem. B* **2002**, *106*, 6129. (c) Babel, A.; Jenekhe, S. A. *J. Phys. Chem. B* **2003**, *107*, 1749.

(8) (a) Sapp, S. A.; Sotzing, G. A.; Reynolds, J. R. *Chem. Mater.* **1998**, *10*, 2101. (b) Fungo, F.; Jenekhe, S. A.; Bard, A. J. *Chem. Mater.* **2003**, *15*, 1264.

(9) Zhang, X.; Kale, D. M.; Jenekhe, S. A. *Macromolecules* **2002**, *35*, 382.

(10) Chen, X. L.; Jenekhe, S. A. *Macromolecules* **1997**, *30*, 1728.

(11) Jenekhe, S. A.; de Paor, L. R.; Chen, X. L.; Tarkka, R. M. *Chem. Mater.* **1996**, *8*, 2401.

(12) (a) Jenekhe, S. A.; Osaheni, J. A. *Science* **1994**, *265*, 765. (b) Osaheni, J. A.; Jenekhe, S. A. *Macromolecules* **1994**, *27*, 739. (c) Gebler, D. D.; Wang, Y. Z.; Blatchford, J. W.; Jessen, S. W.; Fu. D. K.; Swager, T. M.; MacDiarmid, A. G.; Epstein, A. J. *Appl. Phys. Lett.* **1997**, *70*, 1644. (d) Alam, M. M.; Jenekhe, S. A. *J. Phys. Chem. B* **2001**, *105*, 2479.

(13) (a) Berggren, M.; Inganas, O.; Gustafsson, G.; Rasmusson, J.; Andersson, M. R.; Hjertberg, T.; Wennerstrom, O. *Nature (London)* **1994**, *372*, 444. (b) Yu. G.; Nishino, H.; Heeger, A. J.; Chen, T.-A.; Rieke, R. D. *Synth. Met.* **1995**, *72*, 249. (c) Lee, J.-I.; Kang, I.-N.; Hwang, D.-H.; Shim, H.-K. *Chem. Mater.* **1996**, *8*, 1925. (d) Zhang, X.; Shetty, A. S.; Jenekhe, S. A. *Proc. SPIE − Int. Soc. Opt. Eng.* **1997**, *3148*, 89.

(14) (a) Chen, X. L.; Jenekhe, S. A. *Appl. Phys. Lett.* **1997**, *70*, 487. (b) Chen, X. L.; Jenekhe, S. A. *Macromolecules.* **1996**, *29*, 6189. (c) Deussen, M.; Scheidler, M.; Bassler, H. *Synth. Met.* **1995**, *73*, 123.

(15) (a) Agrawal, A. K.; Jenekhe, S. A. *Macromolecules* **1993**, *26*, 895. (b) Agrawal, A. K.; Jenekhe, S. A. *Chem. Mater.* **1996**, *8*, 579. (c) Zhu, Y.; Alam, M. M.; Jenekhe, S. A. *Macromolecules* **2002**, *35*, 9844. (d) Tonzola, C. J.; Alam, M. M.; Jenekhe, S. A. *Adv. Mater.* **2002**, *14*, 1086.

(16) The LUMO energy level of POT was estimated by using the known HOMO level (5.1 eV) and our measured optical band gap of about 1.9 eV: LUMO = HOMO − band gap = 5.1 − 1.9 = 3.2 eV. For the HOMO level, see: Onoda, M.; Tada, K.; Zakhidov, A. A.; Yoshino, K. *Thin Solid Films* **1998**, *331*, 76.

(17) (a) Paul, D. R., Newman, S., Eds. *Polymer Blends*; Academic Press: Orlando, FL, 1978. (b) Ultracki, L. A. *Polymer Alloys and Blends*; Hanser Publishers: Munich, 1990. (c) Bates, F. S. *Science* **1991**, *251*, 898.

(18) (a) Yang, C.-J.; Jenekhe, S. A. *Supramol. Sci.* **1994**, *1*, 91. (b) Berlman, I. B. *Energy Transfer Parameters of Aromatic Compounds*; Academic: New York, 1973. (c) Förster, T. In *Modern Quantum Chemistry: Istanbul Lecture*; Sinanoglu, O., Ed.; Academic: New York, 1965; p 93.

(19) Greenham, N. C.; Samuel, I. D. W.; Hayes, G. R.; Phillips, R. T.; Kessener, Y. A. R. R.; Moratti, S. C.; Holmes, A. B.; Friend, R. H. *Chem. Phys. Lett.* **1995**, *241*, 89.

MA0346299